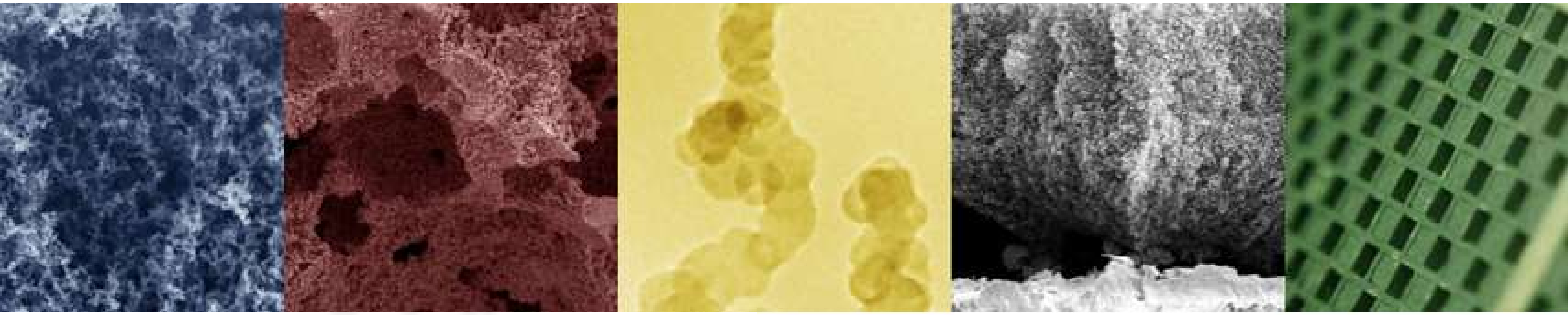

Wall Permeability Estimation in Automotive Particulate Filters

C. Samuels[*1)], S. Aleksandrova[2)], T. C. Watling[3)], H. Medina[4)], S. Benjamin[1)], R. Holtzman[1)]

1) Coventry University, Priory St, Coventry, CV1 5FB, UK
2) University of Leicester, University Rd, Leicester, LE1 7RH
3) Johnson Matthey, Blount's Court, Sonning Common, Reading, RG4 9NH, UK
4) University of Nottingham, Nottingham, NG7 2RD, UK

SiG Meeting – Particulate Matter: Lifecycle and Mitigation

Contact: Samuelsc2@uni.coventry.ac.uk

Johnson Matthey – Inspiring science, enhancing life

University of Leicester

The University of Nottingham

Coventry University

Introduction – Particulate Filters

Fig 1. IC engine exhaust emissions.

- Harmful emissions from IC Engines include particulate matter
- Particulate matter has various detrimental effects:
  - Biological Health
  - Air Quality
  - Global Warming
- New engine technology promoting the production of PM:
  - Direct injection
  - Lean burn
- New regulations reducing particulate emissions (Euro 7 maybe 2025 [1]) leading manufacturers to invest heavily on emissions control.

[1] EURO 7 Commission

Introduction – Particulate Filters

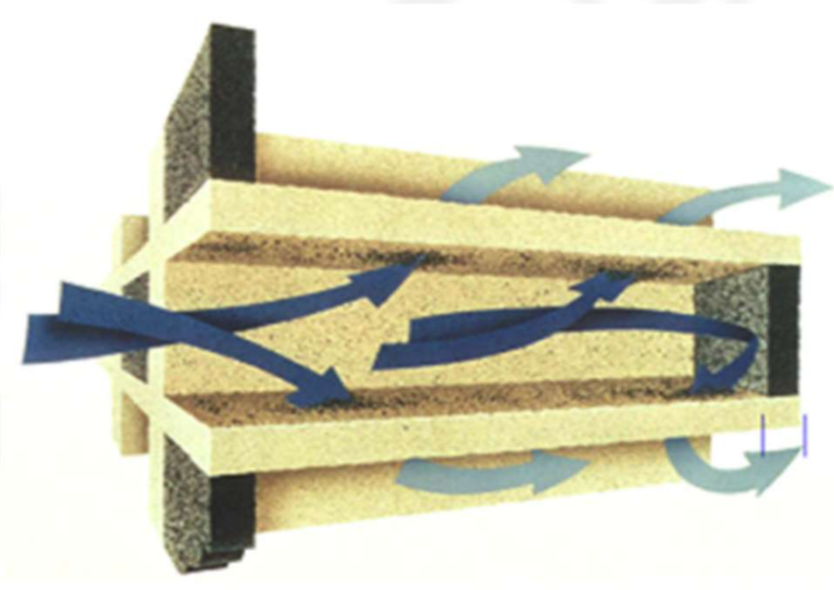

Fig 2. Exhaust gas flow in particulate filter channel [2].

- Emission control:
  - Engine design (EGR, direct-injection)
  - After-treatments (Catalytic converters, Particulate filters)

- Particulate filters
  - Ceramic monolith of square channels
  - Alternate channels blocked
  - PM collection in porous wall
  - PM burned during regeneration

[2] Image from: https://bisaf.co.uk/how-do-dfps-work/

Introduction – Pressure Losses

- Particulate filters cause an increase in exhaust system backpressure
- Need for efficient backpressure prediction models to manage trade-off between filtration efficiency and backpressure
- Backpressure consists of:
  - Frictional losses
  - Contraction/expansion losses
  - Through wall losses

$$\Delta P_{wall} = \frac{\mu}{\boldsymbol{k}} U_{wall} w$$

- Permeability, *k*, needed to predict through wall losses

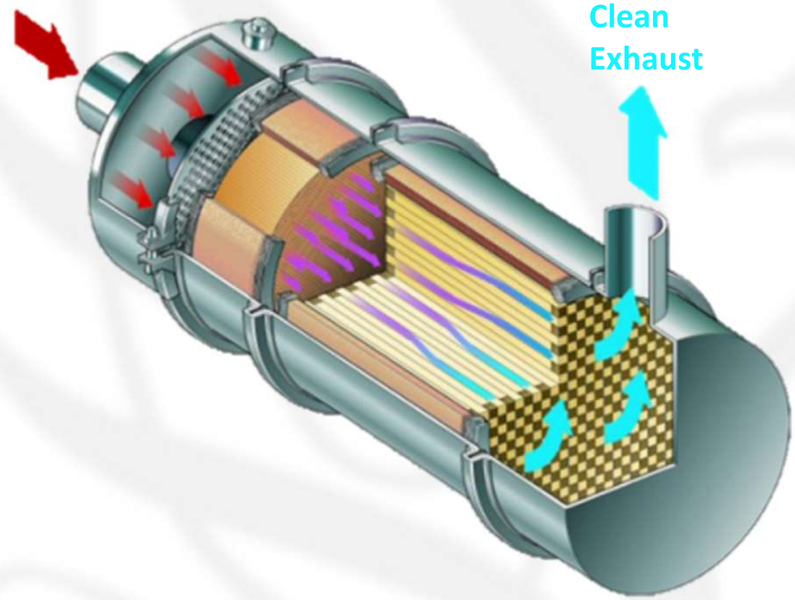

Fig 3. Particulate filter [3].

[3] Image from: McGeehan, et al. 2014 SAE Tech. Paper; doi:10.4271/2014-01-2798

Introduction – Through Wall Losses

- The permeability depends on the medium and flow properties
- Mean Pore Size, **MPS** (μm)
- Porosity, **ε** (%)

$$\epsilon = \frac{Void\ Volume}{Total\ Volume}$$

- Length scale / Charateristic Dimension

$$D = \frac{3(1-\epsilon)}{2\epsilon} MPS$$

- For very complex pore structures like those here, an accurate prediction of the permeability can be a challenge.

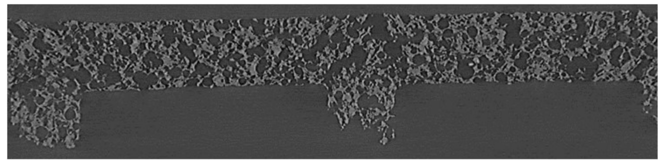

Fig 4. X-ray scan of filter wall

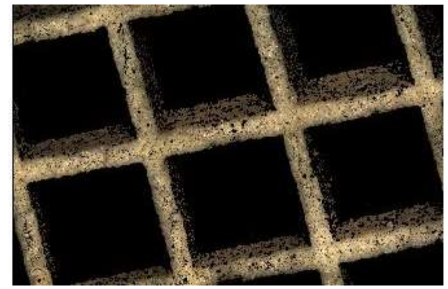

Fig 5. Microscope image of porous monolith

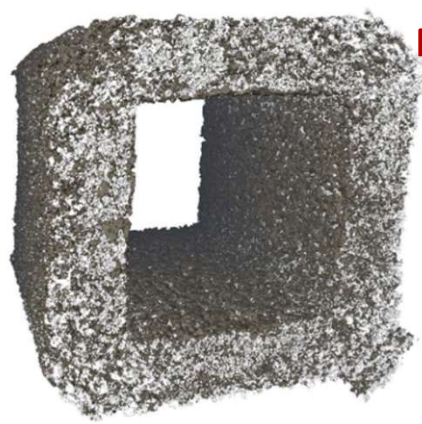

Fig 6. X-ray scan of porous channel [4].

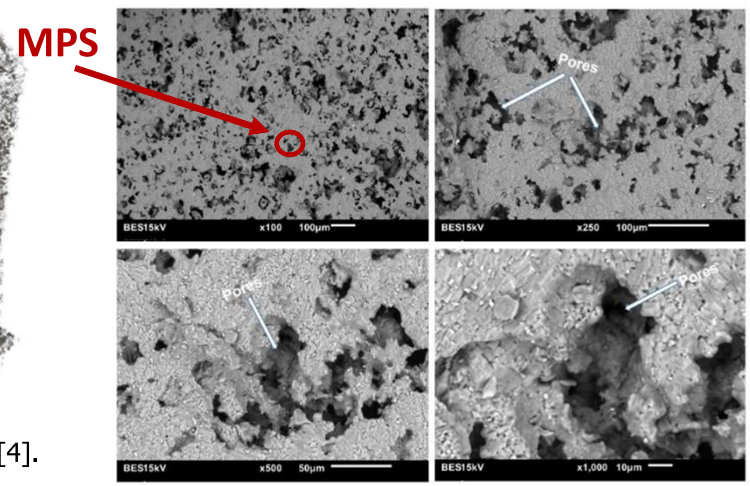

Fig 7. SEM Image of filter wall 100, 50, 10μm [5].

[4] Image from: Kočí, P., 2019, Catalysis Today 320:165-174; doi:10.1016/j.cattod.2017.12.025
[5] Image from: Owolabi, G., 2018, J. Adv. Ceramics, 7:5-16; doi:10.1007/s40145-017-0251-3

Introduction – Permeability Estimation

- Analytical models
  - Semi-empirical expressions - Theoretically derived
  - Simplified medium
  - Based on several assumptions

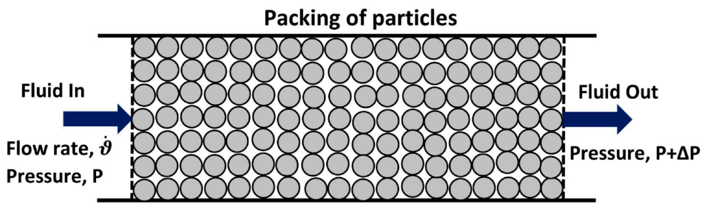

Fig 8. Fluid flow through packed bed [6].

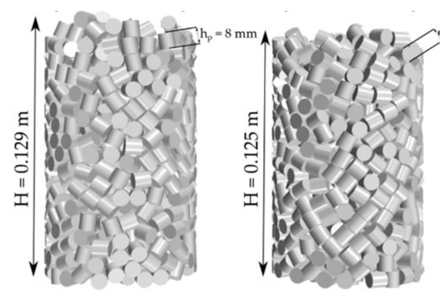

Fig 9. Synthetic generated packing of cylinders [7].

$$k = \frac{2}{9} \times \frac{2 - 1.8(1-\epsilon)^{\frac{1}{3}} - \epsilon - 0.2(1-\epsilon)^2}{1-\epsilon} D^2$$

$$k = \frac{\epsilon^{5.5}}{5.6} D^2$$

$$k = \frac{D^2}{64(1-\epsilon)^{\frac{3}{2}}(1+56(1-\epsilon)^3)}$$

$$k = \frac{\epsilon^3}{k_k(1-\epsilon)^2} D^2$$

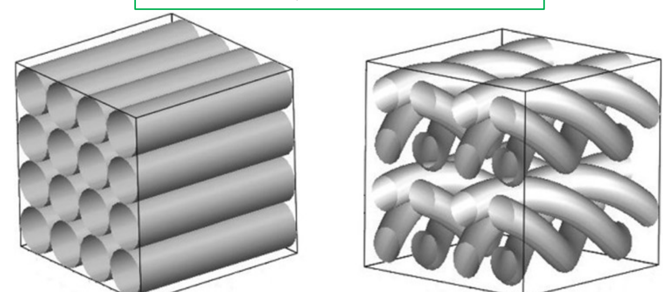

Fig 10. Regular and tortuous bundle of capillaries/tubes [8].

[6] Image from: Pal, R., 2019, Fluids, 4(3), 116; doi:10.3390/fluids4030116
[7] Image from: Flaischlen, S., et al., 2019, ChemEng, 3, 52; doi:10.3390/chemengineering3020052
[8] Image from: Júnior, A., et al., 2021, Trans Porous Media, 138, 99-131; doi:10.1007/s11242-021-01592-4

Introduction – Permeability Estimation

- Curve fitting to core data
  - Pressure drop across core is measured
  - Dependent on model
  - Hard to separate other contributions

Fig 11. Core cut from full size filter.

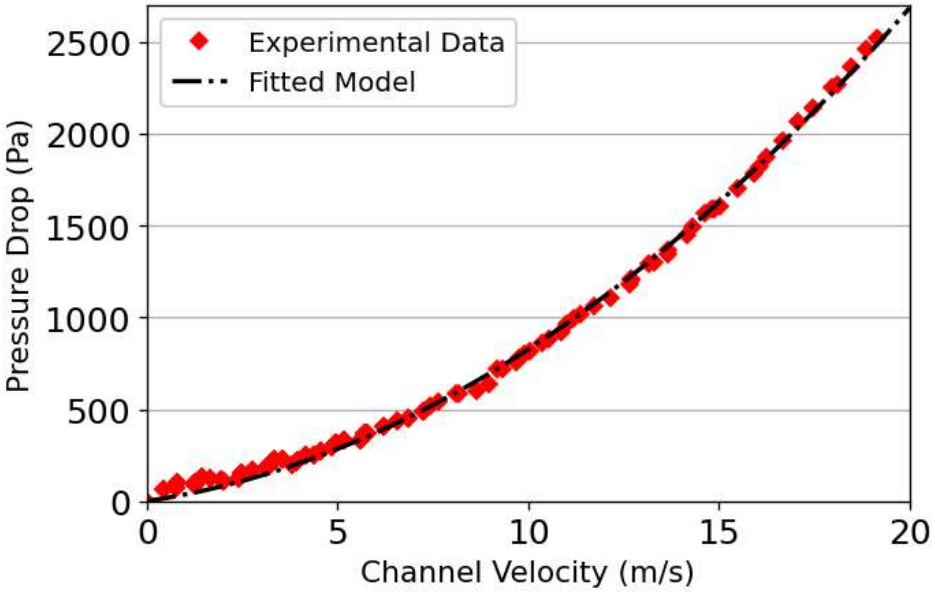

Fig 12. Curve fitting for core data from substrate #2.

Introduction – Permeability Estimation

- Wafer measurements
  - More accurate
  - Time consuming
  - Destructive

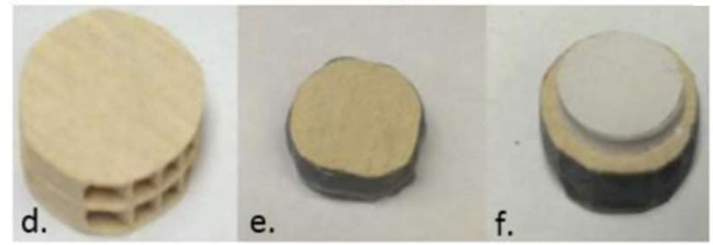

Wafer | Wafer with gasket | Wafer with ash layer

Fig 14. Ash loaded wafers from [9].

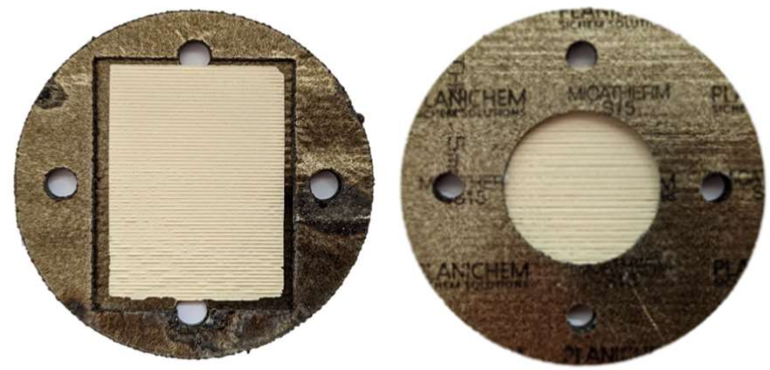

Fig 13. Cutting wafers with piercing saw and wafer sealed in holder

[9] Image from: Kamp, C., et al., 2017, SAE Int. J Fuel Lubr, 10(2):608-618, doi:10.4271/2017-01-0927

Introduction – Permeability Estimation

- Analytical models
  - Semi-empirical expressions - Theoretically derived
  - Simplified medium
  - Based on several assumptions
- Curve fitting to core data
  - Pressure drop across core is measured
  - Dependent on model
  - Hard to separate other contributions
- Wafer measurements
  - More accurate
  - Time consuming
  - Destructive
- Effect of temperature

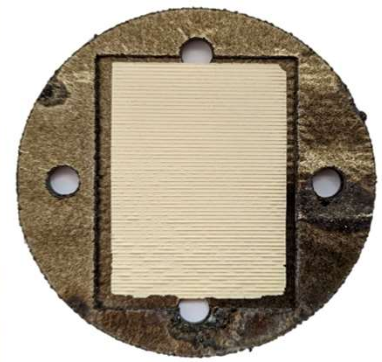

Fig 15. Example of the samples used in this study

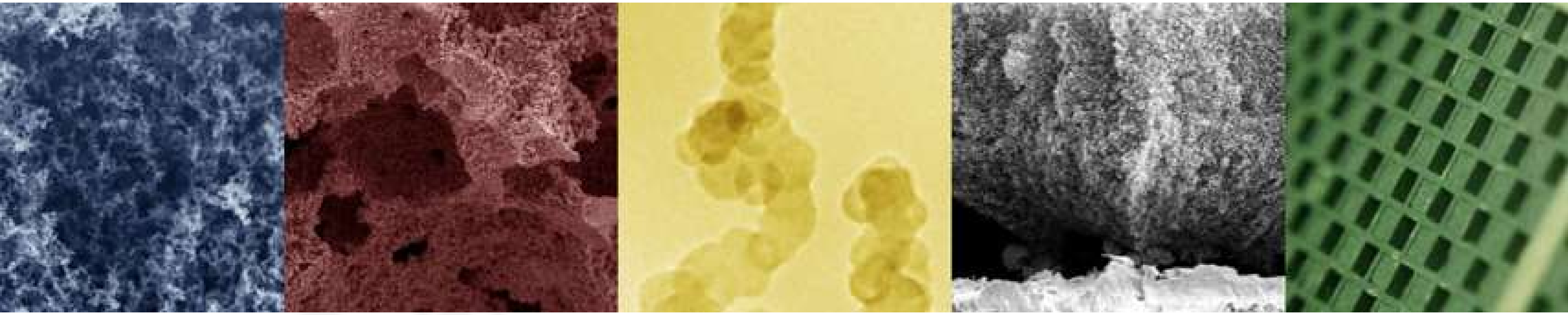

Methodology

Published paper: https://doi.org/10.4271/2023-24-0110

Methodology – Substrates

Table 1. Properties of the substrates used in this study.

#	Material	Mean Pore Size, MPS (µm)	Porosity, ϵ (%)	Wall Thickness, w (mm)	Cells per square inch
1	X	15	49	0.33	300
2	Y	18	65	0.305	300
3	X	17.5	59	0.305	350
4	Y	13	52	0.305	200

Methodology – Sample Preparation

Wafers
- Cutting wafers from full size brick
- Sealing wafers in holder

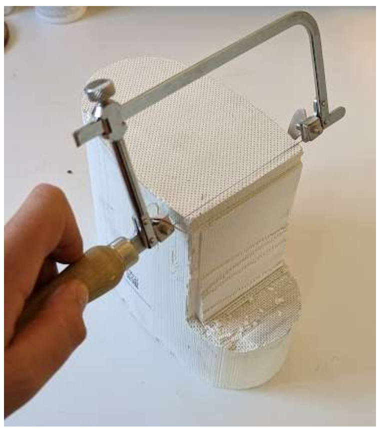

Fig 17. Cutting wafer from full size filter.

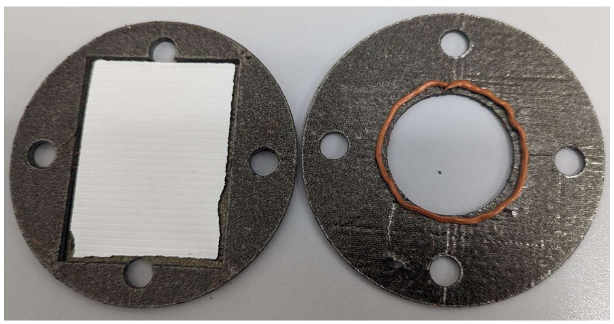

Fig 18. Sealed wafer in sample holder.

Cores
- Cutting cores from full size brick
- Sealing core and mounting in holder

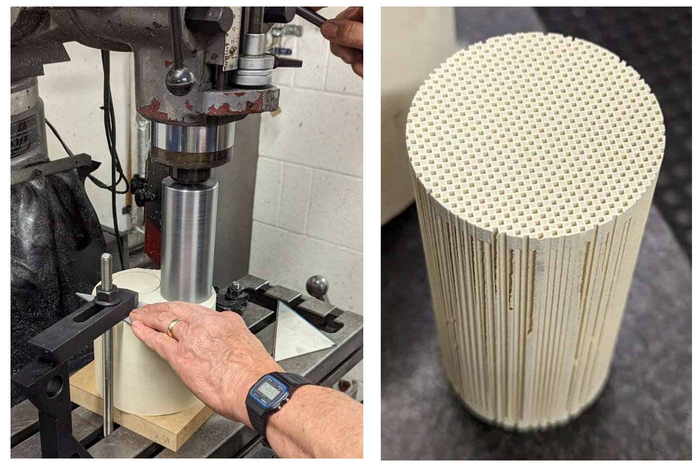

Fig 19. Cutting core from full size filter.

Methodology – Rig Design

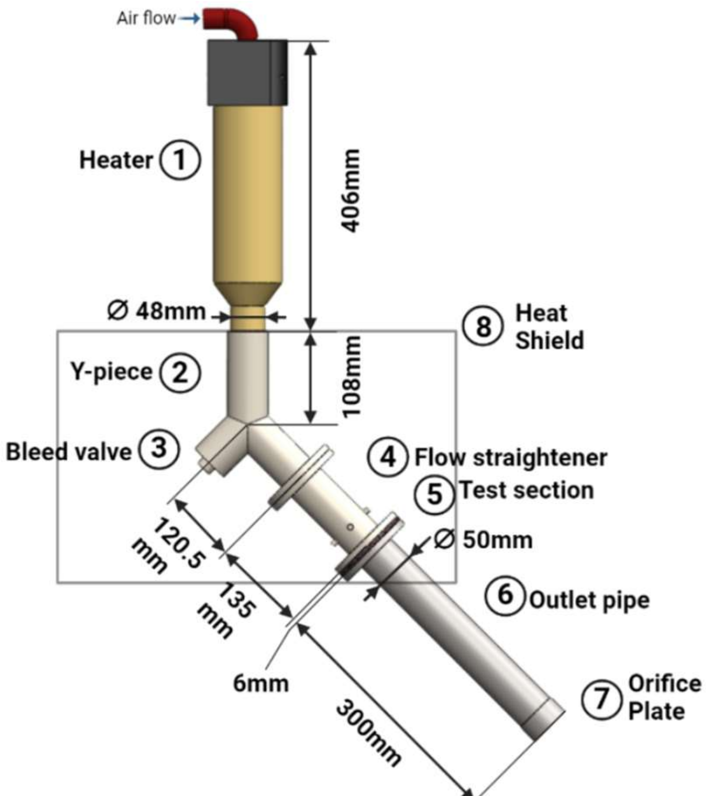

Fig 20. Schematic of flow rig.

WAFERS:
Mass Flow Rate Range: 0 – 1g/s
Wall velocity range:
0 - 0.5m/s

Clean 300/8 filter with diameter 0.12 m and length 0.1 m, this corresponds to around 1500 kg/hr

CORES:
Mass Flow Rate Range:
0 – 130g/s


Fig 21. Experimental flow rigs.

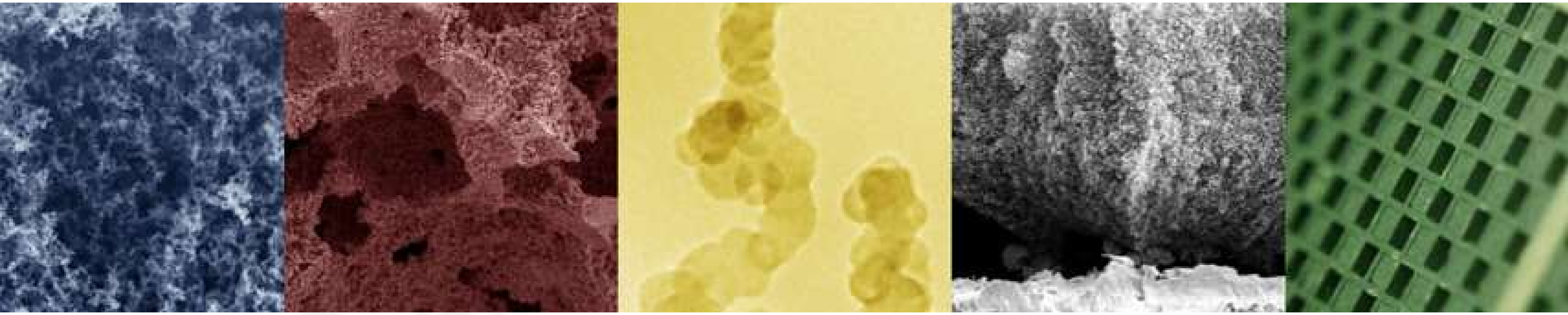

Wafer Results – Cold Flow

Results – Cold Flow

- At least four wafer samples were used for each substrate.
- Spread of data between wafer samples shows good repeatability
- Above 0.15m/s the max deviation from the mean is less than 10%
- Consistent with published results on a different brick with similar properties [10]

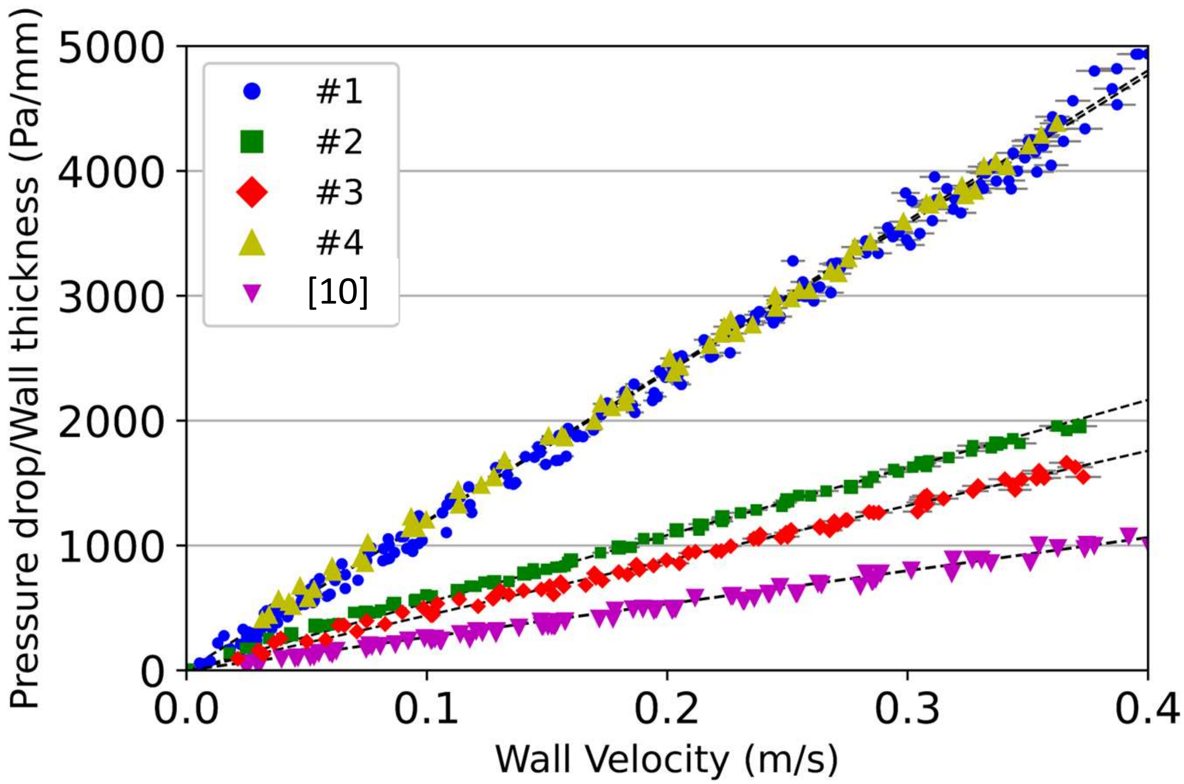

Fig 22. Cold flow test results for all substrates compared with results from [10].

[10] Aleksandrova, et al. 2018 SAE Int. J. Eng., doi:10.4271/03-11-05-0039

Results – Effect of Ridges

To investigate the effect of ridges on wafer samples, 'clean' and 'ridged' wafers were used

Ridged:

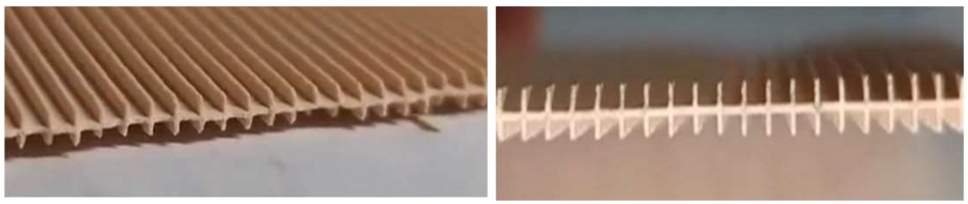

Fig 23. Wafers prepared to maximise ridges

Clean:

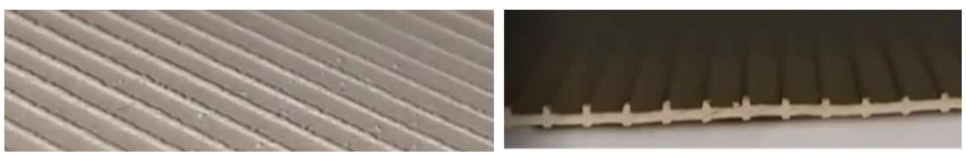

Fig 24. Wafers prepared to minimise ridges

Variation between samples (ridged, clean, normally prepared) was less than 10%. This is consistent with normally prepared wafers and thus the effect of the ridges is neglected.

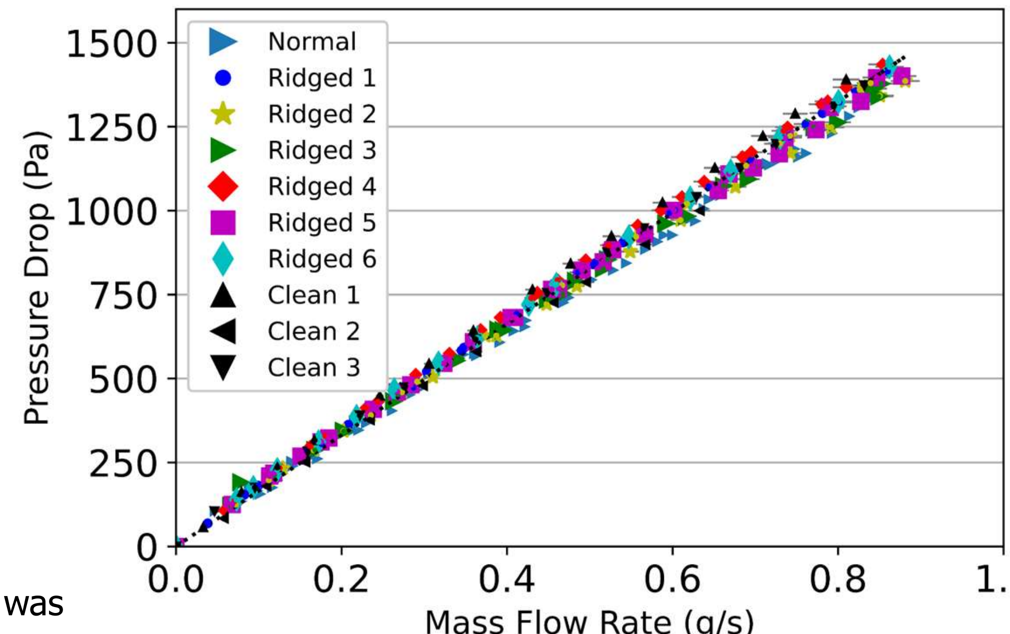

Fig 25. Pressure drop results from ridges study for substrate #1

Results – Permeability

- Using Darcy's Law:

$$\Delta P = \frac{\mu}{k} wU \qquad k = \frac{\mu}{\Delta P} wU$$

$$k = average\ of\ points > 0.15m/s$$

Table 2. Permeability values from cold flow tests

Substrate	k (m^2)
1	1.53×10^{-12}
2	3.41×10^{-12}
3	4.18×10^{-12}
4	1.54×10^{-12}

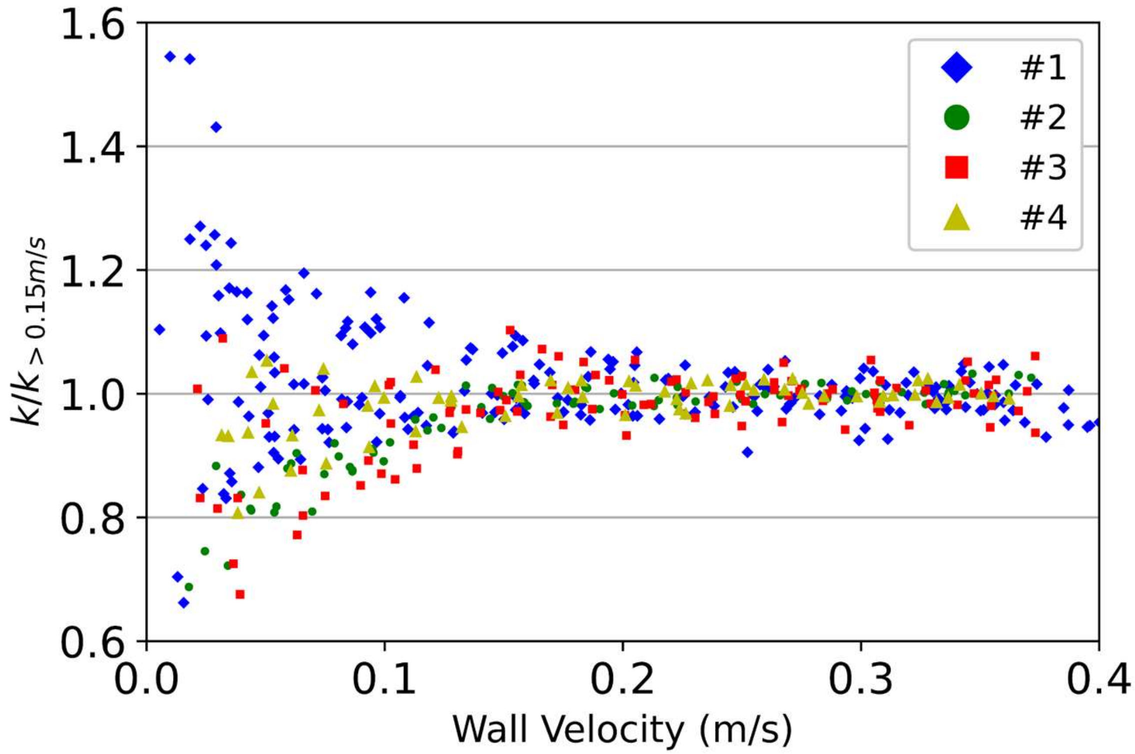

Fig 26. Permeability divided by k_2 for all substrates.

Permeability – Comparison with Analytical Models

Kozeny-Carman [11]

$$k = \frac{\epsilon^3}{C(1-\epsilon)^2} D^2$$

- Classically derived
- Theory [11]: C = 72
- Carman [12]: C = 180
- Ergun [13]: C = 150

Rumpf & Gupte [14]

$$k = \frac{\epsilon^{5.5}}{5.6} D^2$$

- Empirical relationships from packed beds experiments

Kuwabara et al.[15]

$$k = \frac{2}{9} \times \frac{2 - 1.8(1-\epsilon)^{\frac{1}{3}} - \epsilon - 0.2(1-\epsilon)^2}{1-\epsilon} D^2$$

Davies et al. [16]

$$k = \frac{D^2}{64(1-\epsilon)^{\frac{3}{2}}(1+56(1-\epsilon)^3)}$$

- Empirical relationship from fibrous beds experiments

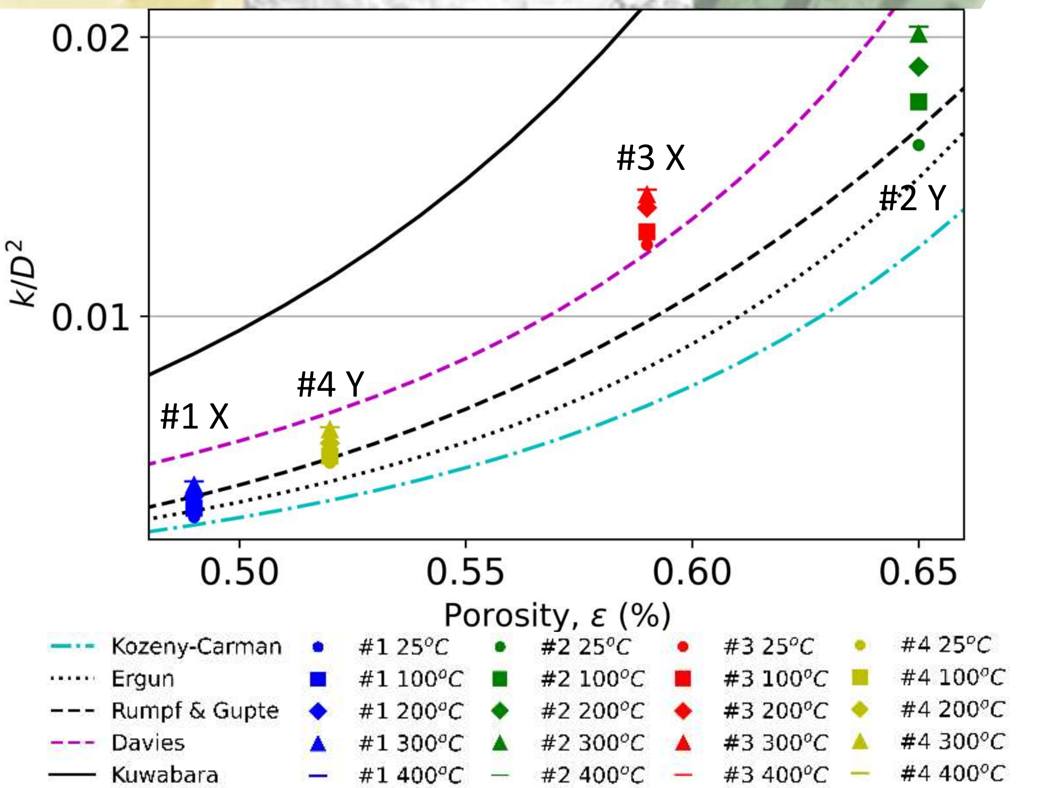

Fig 27. Non-dimensional measured permeability vs porosity with analytical models.

[11] Kozeny, J., 1927, Sitzungsber Akad. Wiss, Wien, 136(2a):271-306
[12] Carman, P., 1937, Inst. Chem. Eng., 15:150-166
[13] Ergun, S., 1949, Ind. Eng. Chem., 41(6):1179-1184
[14] Rumpf, H., 1971, Chem. Ing. Tech., 43(6):367-375
[15] Kuwabara, S., 1959, J. Phys. Soc. Japan, 14:527-532
[16] Davies, C., 1953, IMechE Proceedings, 167(1b):185-213

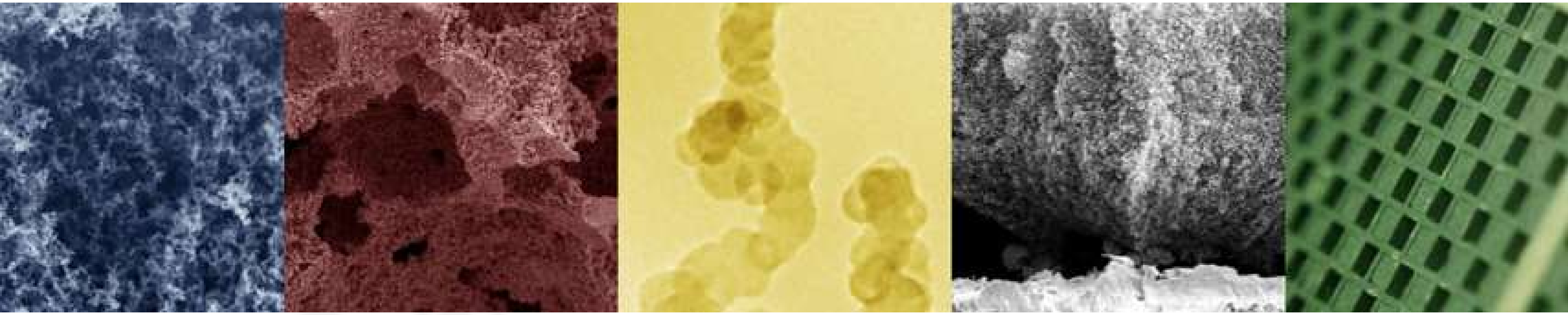

Core Results – Cold Flow

Permeability – Comparison with Core Testing

MODELLING EQUATIONS USING KONST. 0D model from [17]

$$\Delta P_{friction} = \frac{2\mu F L}{3 d_h^2} U$$

$$\Delta P_{contr/expan} = \zeta \frac{\rho}{2} U^2$$

APPROACH1 – LINEAR FITTING

$$\Delta P' = \Delta P_{core} - \Delta P_{friction} - \Delta P_{contr} - \Delta P_{expan}$$

$$\Delta P' = \alpha U \quad \rightarrow \quad k = \frac{\mu}{\alpha} \frac{d_h w}{4L}$$

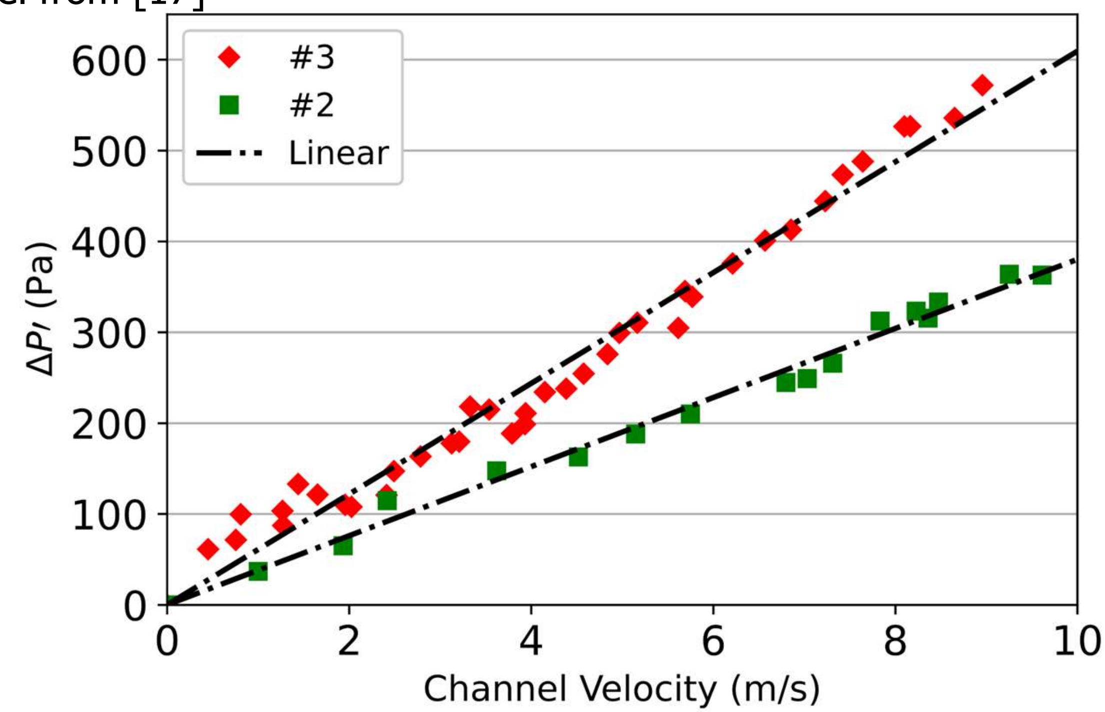

Fig 28. Linear curve fitting for substrates #2 and #3.

[17] Konstandopoulos, G.,1989, SAE Technical Paper 890405; doi:10.4271/890405

Permeability – Comparison with Core Testing

MODELLING EQUATIONS USING KONST. 0D model from [19]

$$\Delta P_{friction} = \frac{2\mu F L}{3 d_h^2} U$$

$$\Delta P_{contr/expan} = \zeta \frac{\rho}{2} U^2$$

APPROACH 2 – QUADRATIC FITTING

$$\Delta P'' = \Delta P_{core} - \Delta P_{friction}$$

$$\Delta P'' = \alpha U + \beta U^2 \quad \rightarrow k = \frac{\mu}{\alpha}\frac{d_h w}{4L}$$

$$\zeta = \frac{2\beta}{\rho}$$

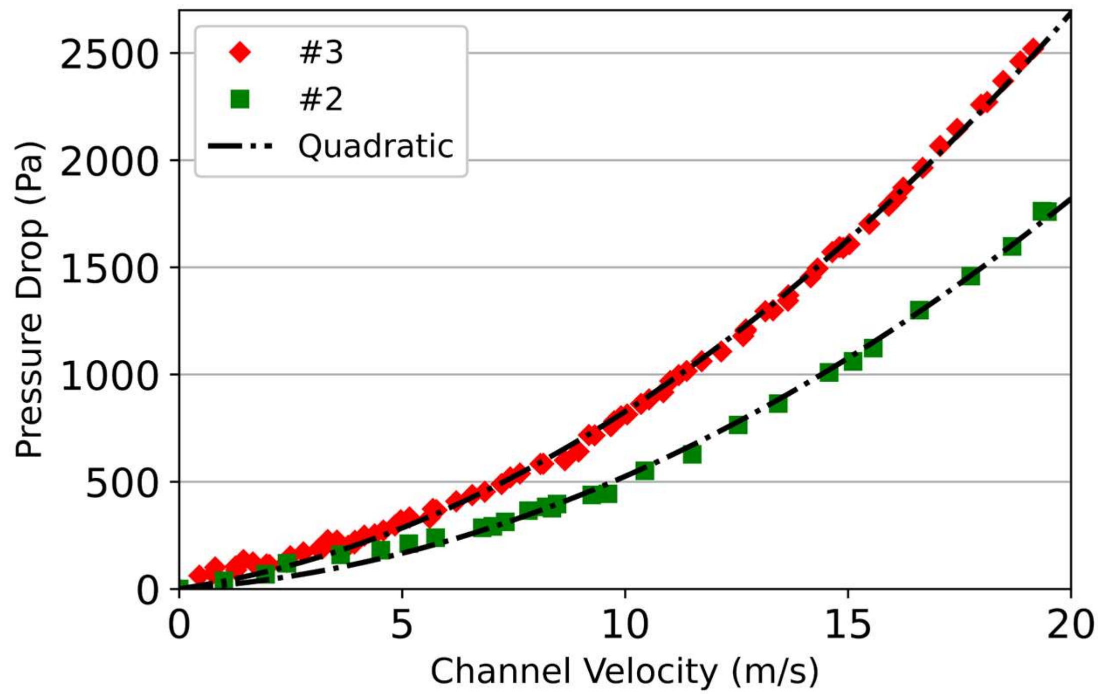

Fig 29. Quadratic curve fitting for substrates #2 and #3.

[17] Konstandopoulos, G.,1989, SAE Technical Paper 890405; doi:10.4271/890405

Permeability – Comparison with Core Testing

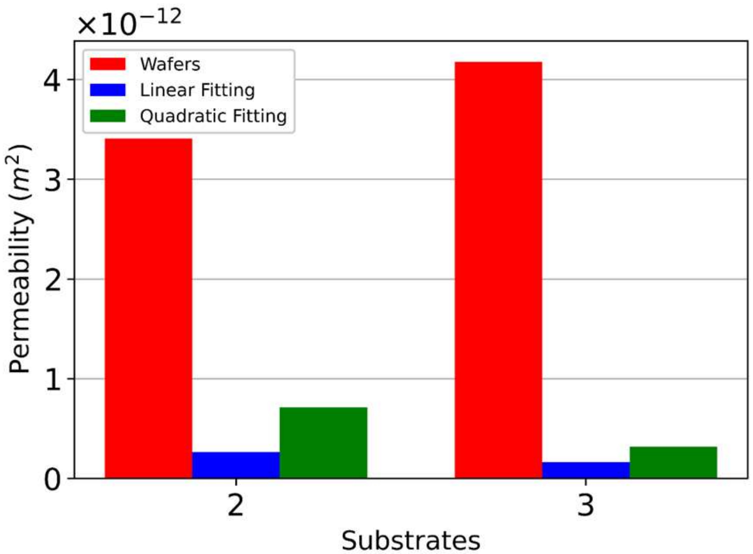

Fig 30. Permeability derived from core testing comparison with wafers

- Considerable difference to k calculated with wafer experiments (at least an order of magnitude)
- Heavy reliance on the models and its assumptions
- Sensitive to Reynolds number/velocity range used for fitting

Table 3. k_1 and k_2 values from cold flow tests

Substrate	#2		#3	
Method	k (m²)	ζ	k (m²)	ζ
Wafers	3.41×10^{-12}		4.18×10^{-12}	
Linear	2.63×10^{-13}		1.62×10^{-13}	
Quadratic	7.13×10^{-13}	6.4	3.19×10^{-13}	9.02

[17] Konstandopoulos, G.,1989, SAE Technical Paper 890405; doi:10.4271/890405

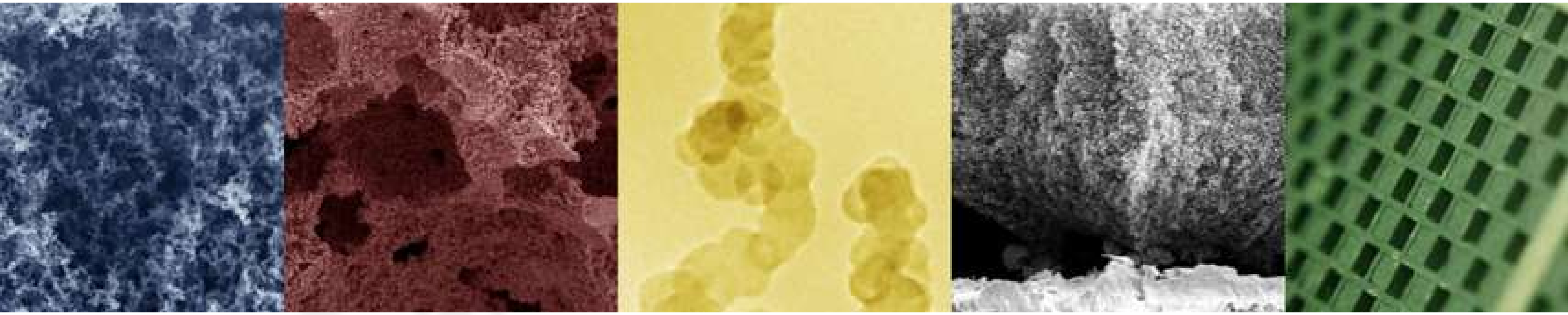

Wafer Results – Hot Flow

Results – Hot Flow

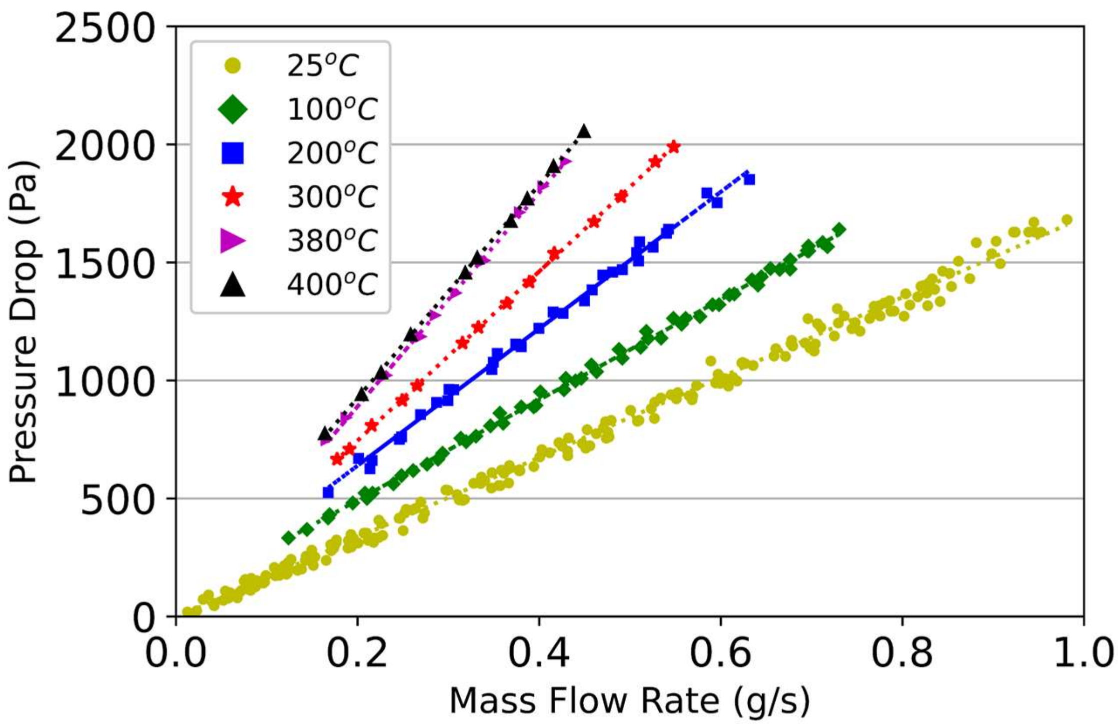

Fig 31. Hot flow pressure drop results for substrate #1.

- Temperature up to 400°C
- Pressure drop increases as expected with temperature – increasing the contribution of the through-wall losses to the total pressure drop.
- Reduction in flow rate range due to increased pressure leading to earlier wafer breakage

Permeability – Hot Flow

- Permeability normalised by value of k at 25^{o}C
- Permeability increase with temperature by at least 15% for all substrates at 400^{o}C and up to 45% for substrate #1
- Findings consistent with published results from [10]
- Slip effect more pronounced than usually assumed (see [10])
- For exhaust gas temperatures that reach up to 900^{o}C, the extent of this effect could be even greater. More testing to higher temperatures is needed.

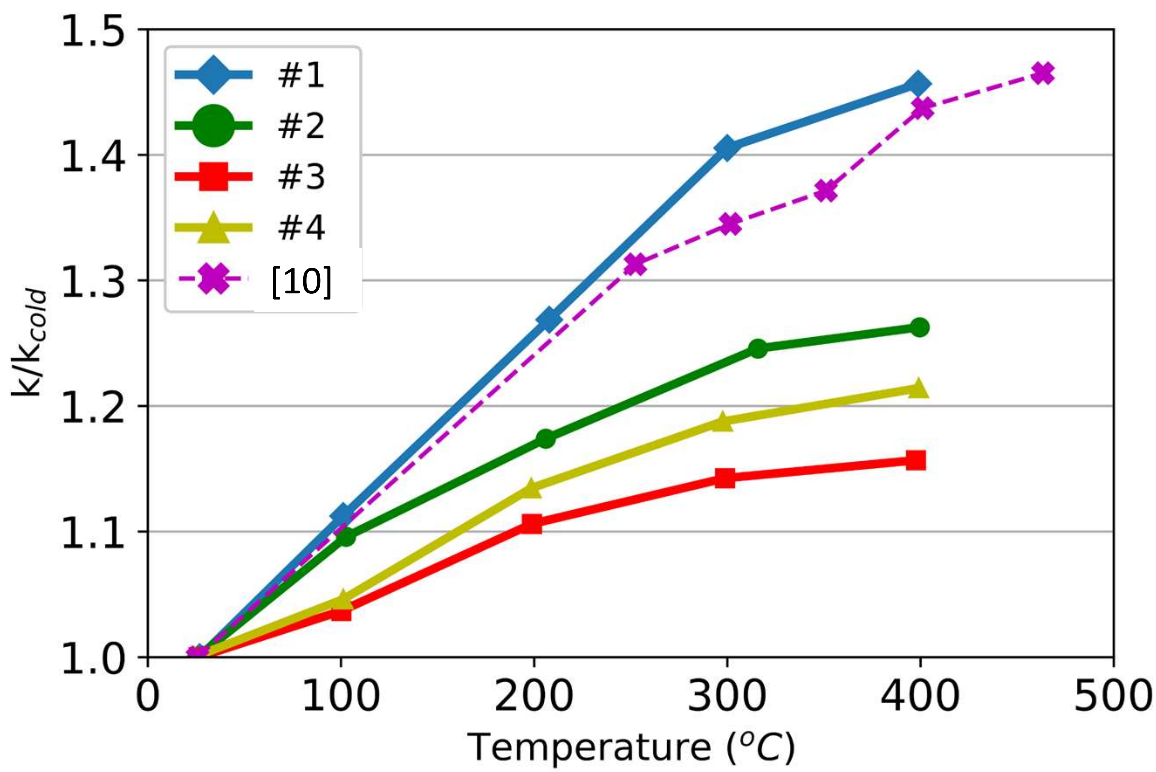

Fig 32. Scaled permeability (k/k_{cold}) vs temperature

[10] Aleksandrova, et al. 2018 SAE Int. J. Eng., doi:10.4271/03-11-05-0039

Slip Effect – Modelling

Knudsen number: $Kn = \frac{\lambda}{D}$

- Where **λ** is the **free mean path** of the gas molecule and **D** is the **characteristic length**
- λ increases with temperature (gas rarefication)
- Kn > 0.01 are considered to be in the slip flow regime

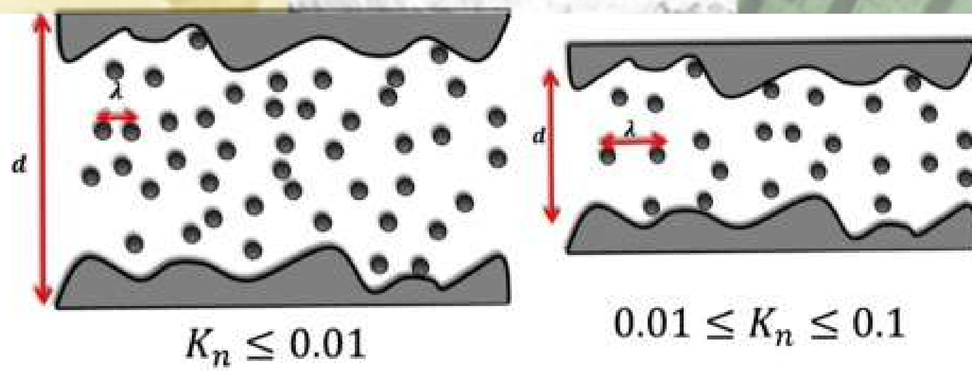

Fig 35. Schematic of flow regimes with different mean free path and pore size [18]

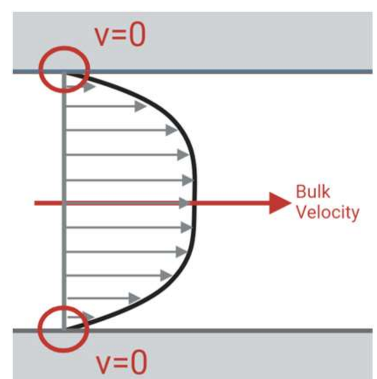

Fig 33. No-slip boundary condition

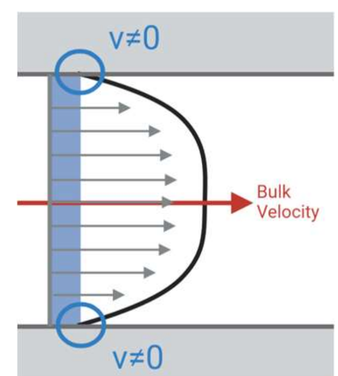

Fig 34. Slip boundary condition

[18] Moghaddam, R., et al. 2016, Fuel 173:298-310; doi:10.1016/j.fuel.2016.01.057

Slip Effect – Modelling

Knudsen number: $Kn = \frac{\lambda}{D}$

- Where **λ** is the **free mean path** of the gas molecule and **D** is the **characteristic length**
- λ increases with temperature (gas rarefication)
- Kn > 0.01 are considered to be in the slip flow regime

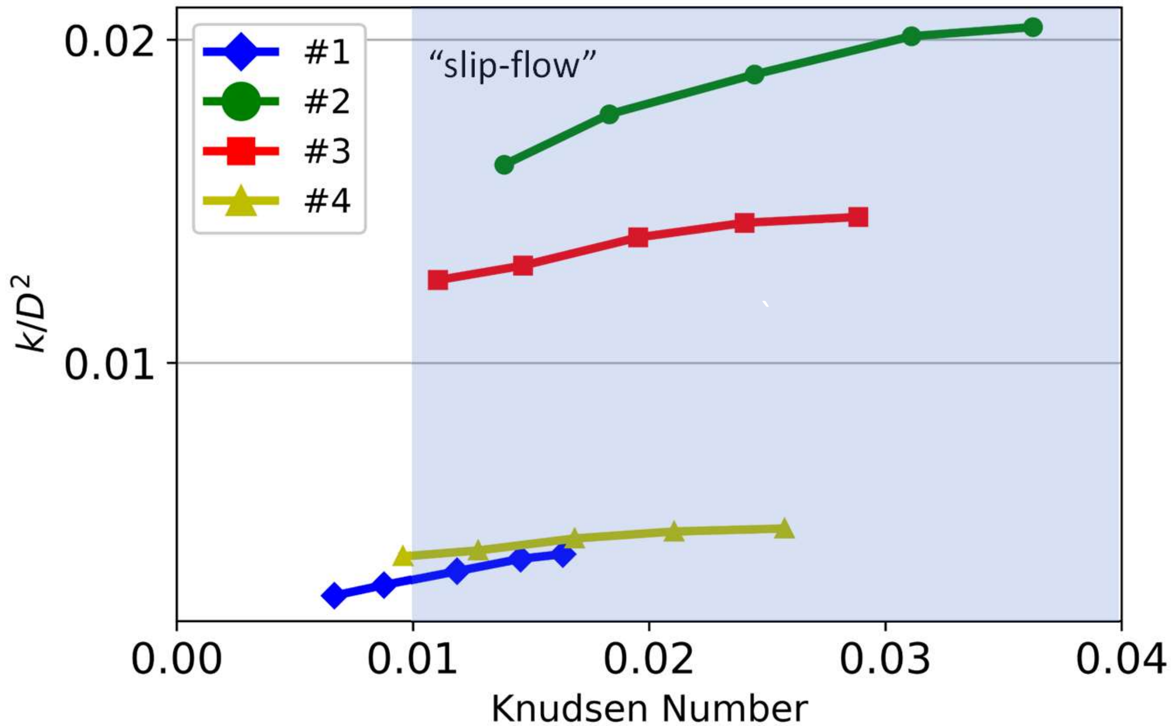

Fig 36. Normalised permeability vs Knudsen number

[18] Moghaddam, R., et al. 2016, Fuel 173:298-310; doi:10.1016/j.fuel.2016.01.057

Slip Effect – Modelling

Lee et al. [19]

$$k = \frac{2(K_1 + 3K_2\sigma_v Kn)}{9(1-\epsilon)(1+2\sigma_v Kn)}\frac{D^2}{4}$$

Where:

$$K_1 = 2 - \frac{9}{5}(1-\epsilon)^{\frac{1}{3}} - \epsilon - \frac{1}{5}(1-\epsilon)^2$$

$$K_2 = 1 - \frac{6}{5}(1-\epsilon)^{\frac{1}{3}} + \frac{1}{5}(1-\epsilon)^2$$

Using Stokes-Cunningham Factor [17]

$$\frac{k}{k_0} = SCF = 1 + Kn(1.257 + 0.4e^{-\frac{1.1}{Kn}})$$

Maxwell et al. [18] with C1 from [10]

$$\frac{k}{k_0} - 1 = 4C_1 Kn$$

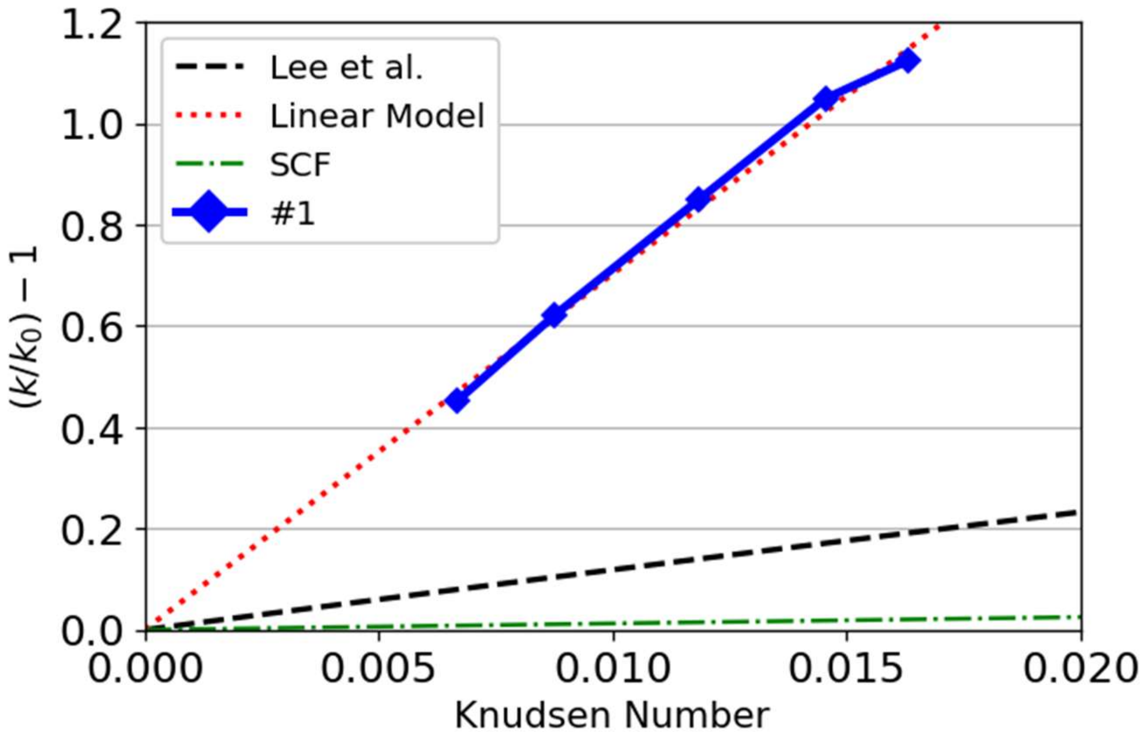

Fig 37. Comparison with slip models for substrate #1

[10] Aleksandrova, et al. 2018 SAE Int. J. Eng., doi:10.4271/03-11-05-0039
[17] Konstandopoulos, 1989, SAE Technical Paper 890405; doi:10.4271/890405
[18] Moghaddam, R., et al. 2016, Fuel 173:298-310; doi:10.1016/j.fuel.2016.01.057
[19] Lee, K., et al., 1978, J. Aerosol Sci., 9(6):557-565; doi:10.1016/0021-8502(78)90021-6

Slip Effect – Modelling

Lee et al. [19]

$$k = \frac{2(K_1 + 3K_2\sigma_v Kn)}{9(1-\epsilon)(1+2\sigma_v Kn)}\frac{D^2}{4}$$

Where:

$$K_1 = 2 - \frac{9}{5}(1-\epsilon)^{\frac{1}{3}} - \epsilon - \frac{1}{5}(1-\epsilon)^2$$

$$K_2 = 1 - \frac{6}{5}(1-\epsilon)^{\frac{1}{3}} + \frac{1}{5}(1-\epsilon)^2$$

Using Stokes-Cunningham Factor [17]

$$\frac{k}{k_0} = SCF = 1 + Kn(1.257 + 0.4e^{-\frac{1.1}{Kn}})$$

Maxwell et al. [18] with C1 from [10]

$$\frac{k}{k_0} - 1 = 4C_1 Kn$$

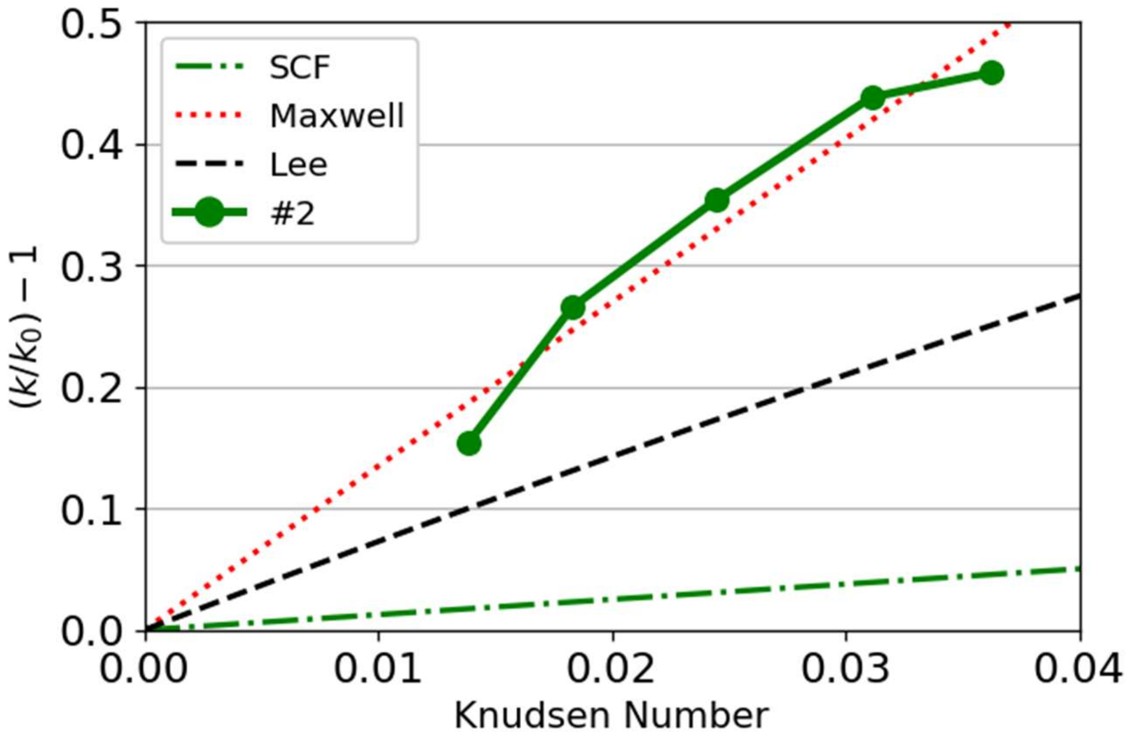

Fig 38. Comparison with slip models for substrate #2

[10] Aleksandrova, et al. 2018 SAE Int. J. Eng., doi:10.4271/03-11-05-0039
[17] Konstandopoulos, 1989, SAE Technical Paper 890405; doi:10.4271/890405
[18] Moghaddam, R., et al. 2016, Fuel 173:298-310; doi:10.1016/j.fuel.2016.01.057
[19] Lee, K., et al., 1978, J. Aerosol Sci., 9(6):557-565; doi:10.1016/0021-8502(78)90021-6

Slip Effect – Modelling

Lee et al. [19]

$$k = \frac{2(K_1 + 3K_2\sigma_v Kn)}{9(1-\epsilon)(1+2\sigma_v Kn)}\frac{D^2}{4}$$

Where:

$$K_1 = 2 - \frac{9}{5}(1-\epsilon)^{\frac{1}{3}} - \epsilon - \frac{1}{5}(1-\epsilon)^2$$

$$K_2 = 1 - \frac{6}{5}(1-\epsilon)^{\frac{1}{3}} + \frac{1}{5}(1-\epsilon)^2$$

Using Stokes-Cunningham Factor [17]

$$\frac{k}{k_0} = SCF = 1 + Kn(1.257 + 0.4e^{-\frac{1.1}{Kn}})$$

Maxwell et al. [18] with C1 from [10]

$$\frac{k}{k_0} - 1 = 4C_1 Kn$$

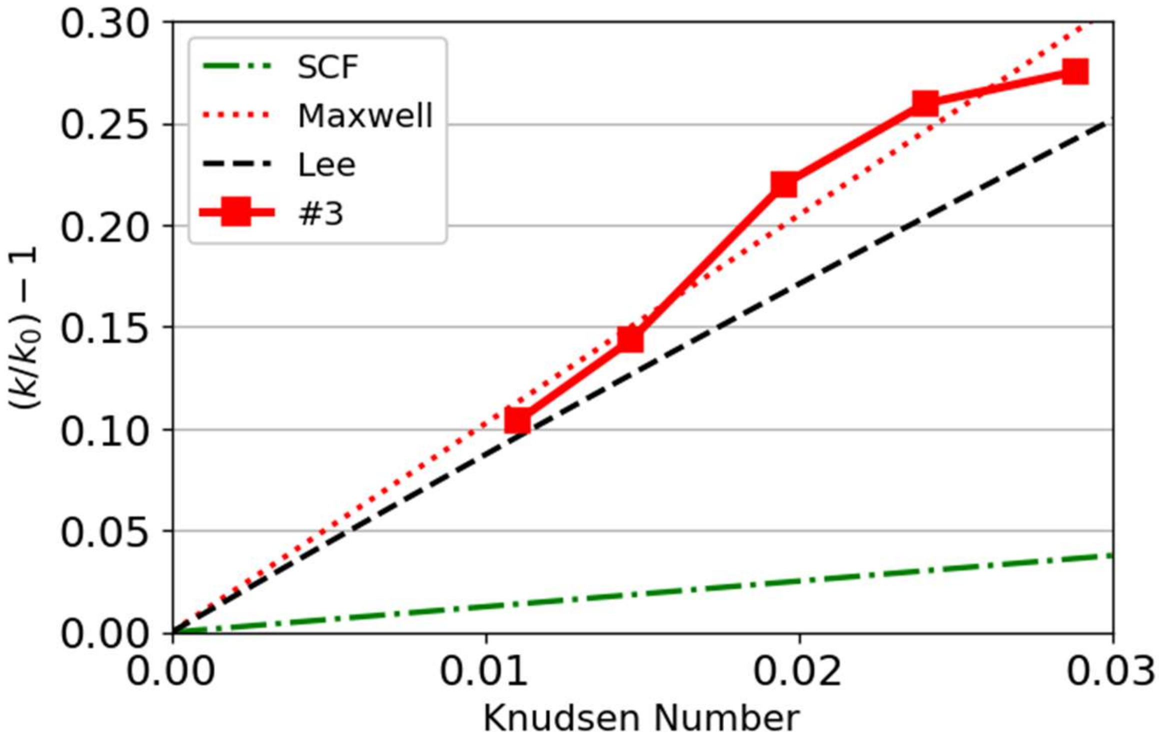

Fig 39. Comparison with slip models for substrate #3

[10] Aleksandrova, et al. 2018 SAE Int. J. Eng., doi:10.4271/03-11-05-0039
[17] Konstandopoulos, 1989, SAE Technical Paper 890405; doi:10.4271/890405
[18] Moghaddam, R., et al. 2016, Fuel 173:298-310; doi:10.1016/j.fuel.2016.01.057
[19] Lee, K., et al., 1978, J. Aerosol Sci., 9(6):557-565; doi:10.1016/0021-8502(78)90021-6

Slip Effect – Modelling

Lee et al. [19]

$$k = \frac{2(K_1 + 3K_2\sigma_v Kn)}{9(1-\epsilon)(1+2\sigma_v Kn)}\frac{D^2}{4}$$

Where:

$$K_1 = 2 - \frac{9}{5}(1-\epsilon)^{\frac{1}{3}} - \epsilon - \frac{1}{5}(1-\epsilon)^2$$

$$K_2 = 1 - \frac{6}{5}(1-\epsilon)^{\frac{1}{3}} + \frac{1}{5}(1-\epsilon)^2$$

Using Stokes-Cunningham Factor [17]

$$\frac{k}{k_0} = SCF = 1 + Kn(1.257 + 0.4e^{-\frac{1.1}{Kn}})$$

Maxwell et al. [18] with C1 from [10]

$$\frac{k}{k_0} - 1 = 4C_1 Kn$$

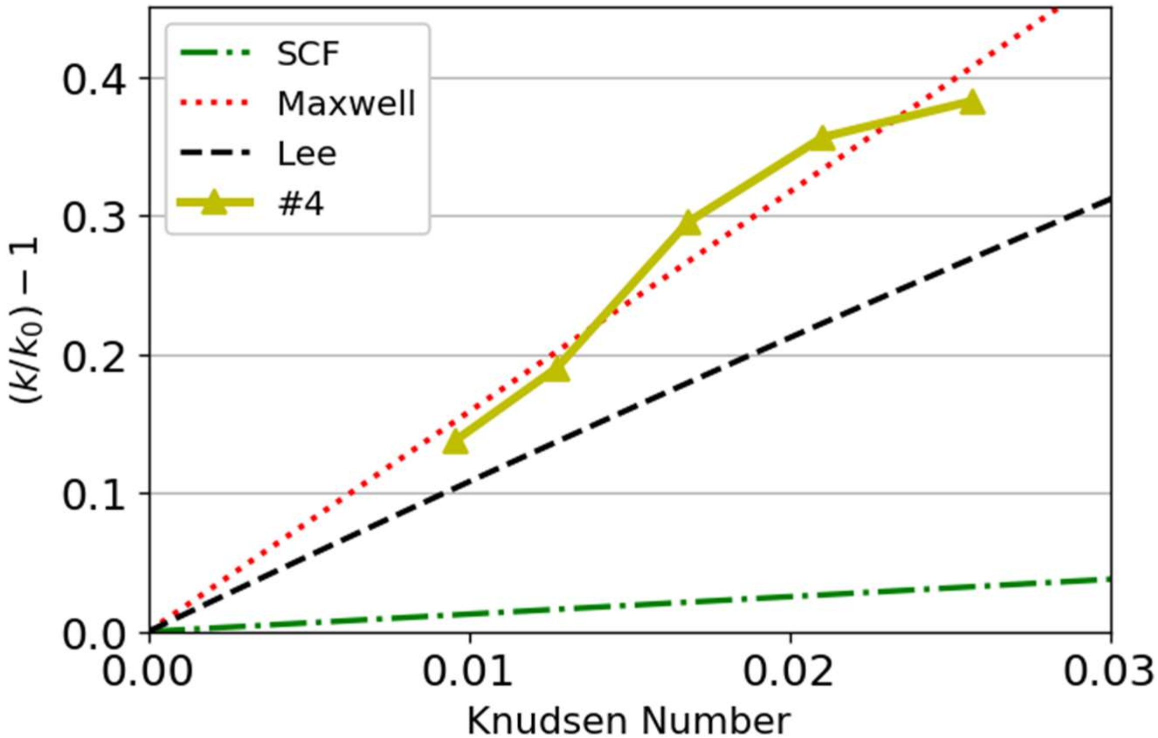

Fig 40. Comparison with slip models for substrate #4

[10] Aleksandrova, et al. 2018 SAE Int. J. Eng., doi:10.4271/03-11-05-0039
[17] Konstandopoulos, 1989, SAE Technical Paper 890405; doi:10.4271/890405
[18] Moghaddam, R., et al. 2016, Fuel 173:298-310; doi:10.1016/j.fuel.2016.01.057
[19] Lee, K., et al., 1978, J. Aerosol Sci., 9(6):557-565; doi:10.1016/0021-8502(78)90021-6

Conclusions

- Robust and repeatable methodology for permeability measurement.
- Comparison with analytical estimations shows the limitations of their predictive capabilities.
- The core testing method's accuracy is low (difference by at least an order of magnitude).
- The permeability is shown to increase with temperature, something that has been attributed to the slip effect.
- Existing correlations to predict the effect of slip under predict its contribution considerably.

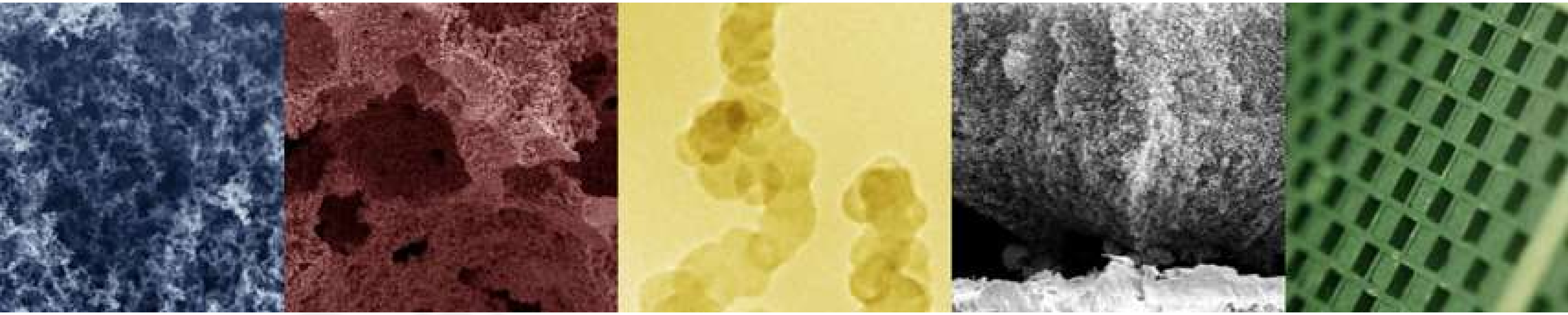

On-going / Future Work

CFD Study on Wafers - Introduction

X-ray Tomography at Johnson Matthey

Fig 41. Section of wafer removed from sample from experiments.

Fig 42. Section of wafer mounted on cocktail stick

Fig 43. Sample inside XRT scanner

CFD Study on Wafers - Introduction

Output: Tiff stack
~ 1700 tiff files
resolution of 2µm

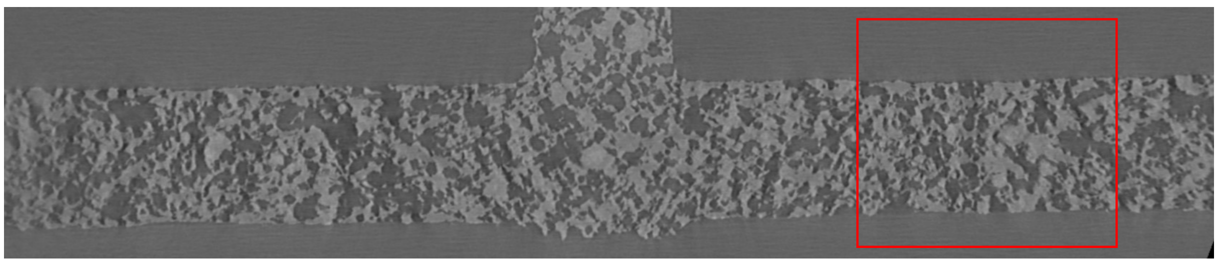

Fig 44. Example of tiff file represented an image slice of the sample.

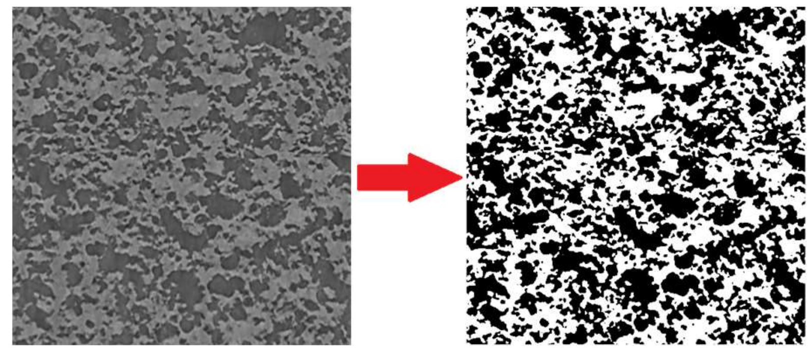

Fig 45. Thresholding the image slices using Otsu algorithm

CFD Study on Wafers – Setup

CFD Methodology:

- Star CCM+
- Incompressible, isothermal, unsteady air flow model
- Laminar flow model
- Adaptive time-step to keep max CFL number < 1

$$CFL = \frac{a\Delta t}{\Delta x}$$

- Velocity Inlet, flow normal to boundary
- Symmetry planes
- Outlet pressure set to atmospheric

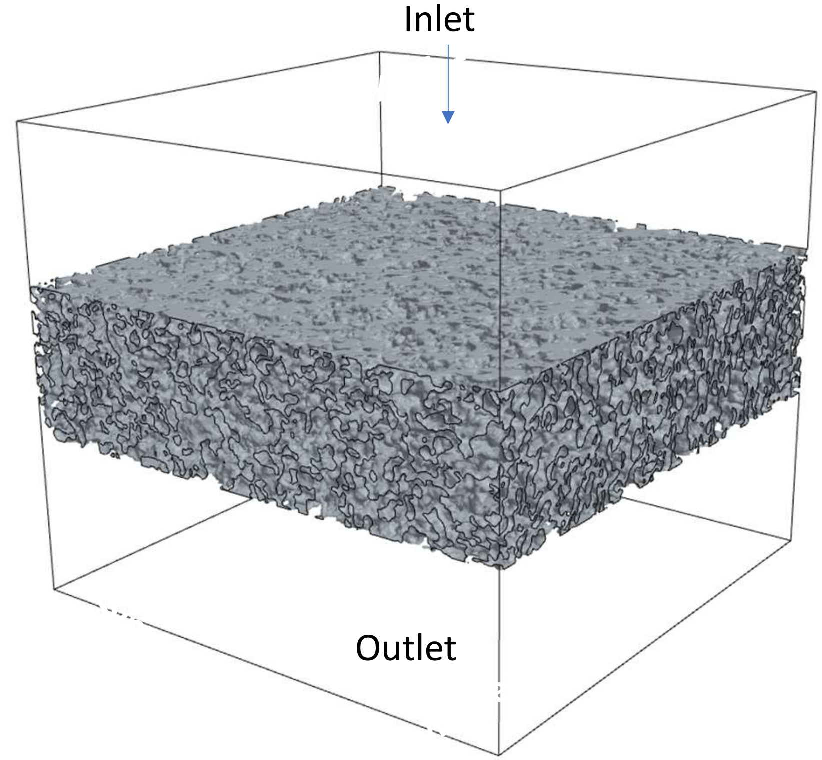

Fig 46. Flow domain in StarCCM+

CFD Study on Wafers - Results

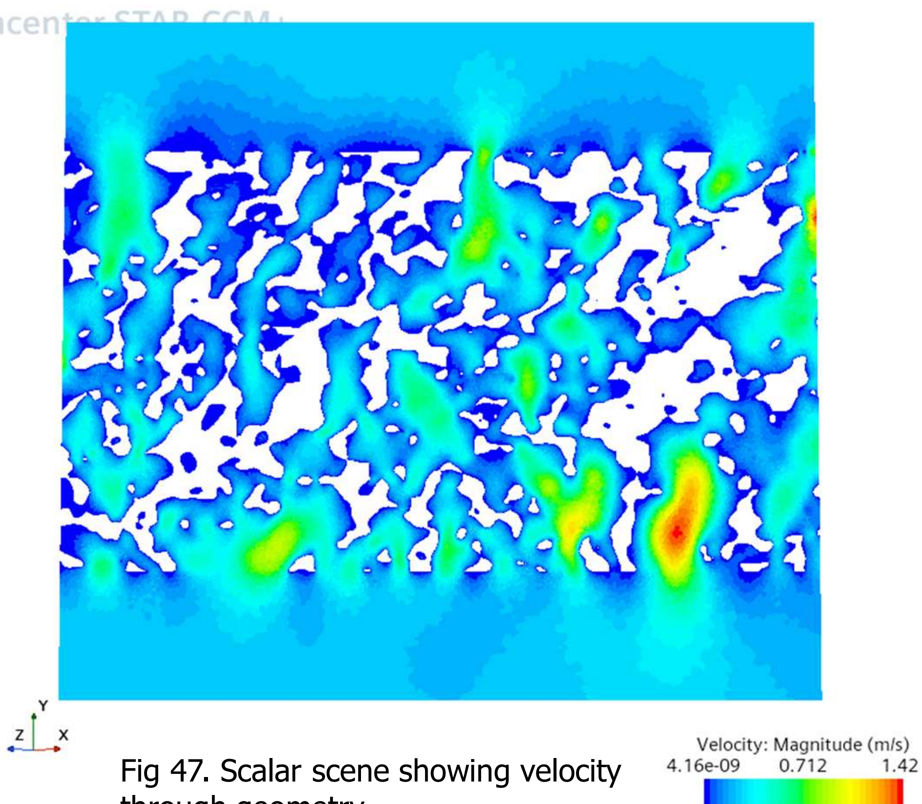

Fig 47. Scalar scene showing velocity through geometry.

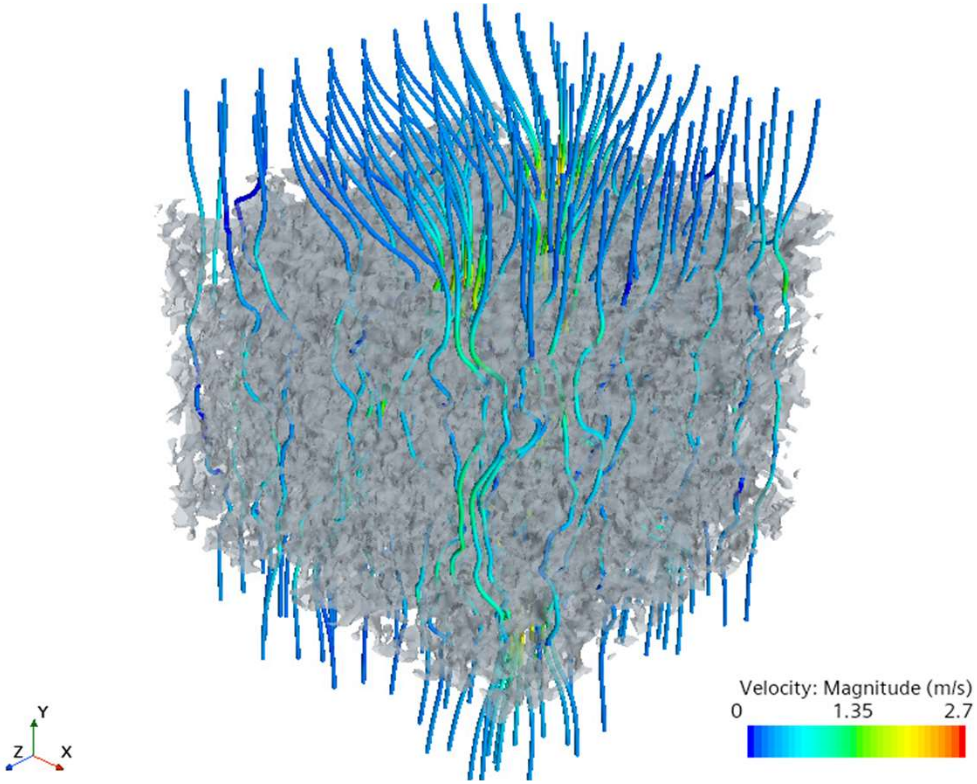

Fig 48. Streamlines through 3D geometry

CFD Study on Wafers - Results

- CFD predict a permeability value almost 3 times higher than that found in the experiments.
- The trend matches experiments, however, the magnitude is out.
- This could result in upto a 40% error in prediction of through-wall losses.

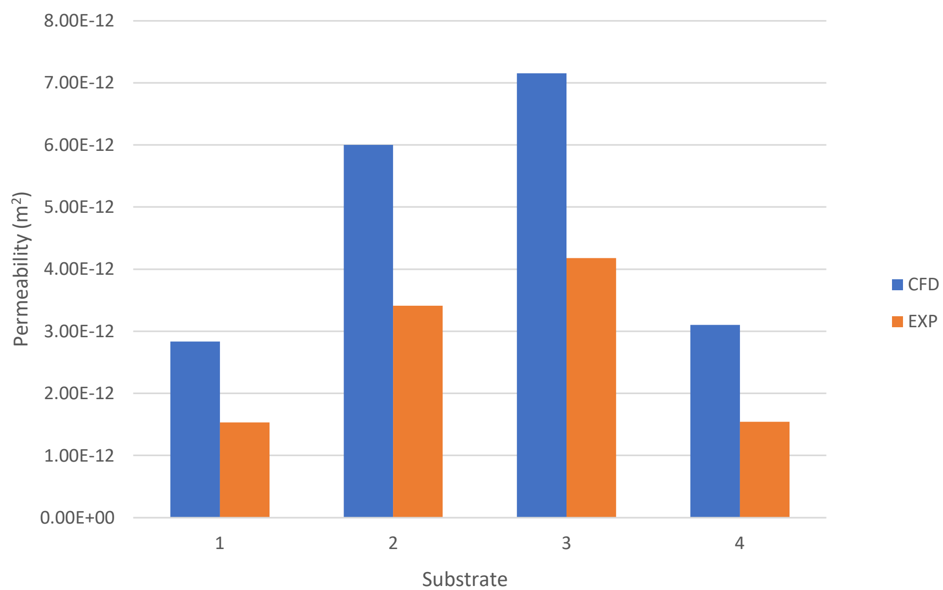

Fig 49. Comparison of permeability from CFD and experiments.

Catalyst Coated Filters

Issues:
1. Uniformity of the coating
2. Coating procedure

Wafer Coating Methods:
1. Dip coating
2. K-bar method

Table 4. Properties of the washcoat used for coated wafers.

#	Composition	D90 Washcoat Particle Size (µm)	Pore Former
1	Al_2O_3	6	-
2	Al_2O_3	10.9	-
3	Al_2O_3	17	-
4	Al_2O_3	6	A
5	Al_2O_3	6	V

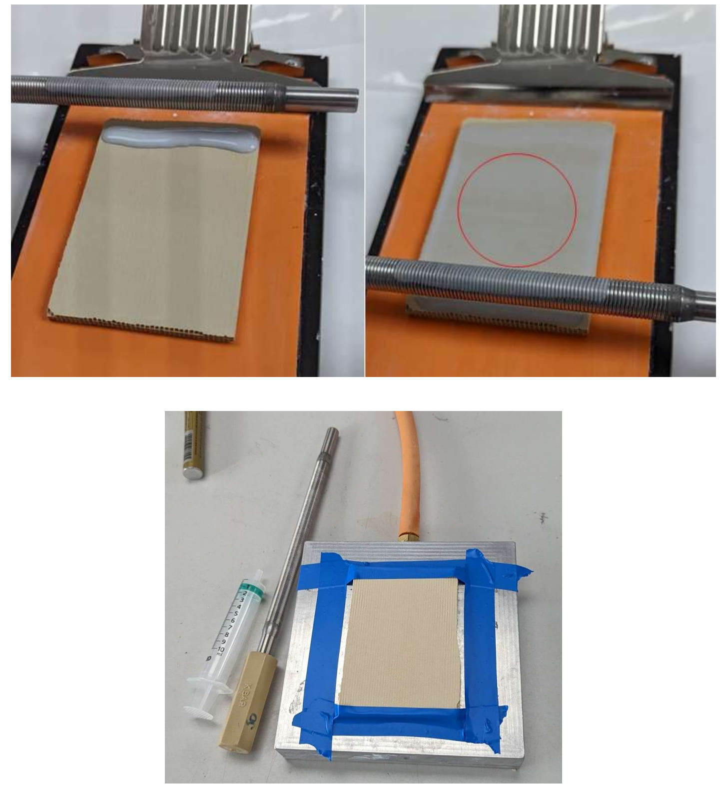

Fig 50. Coating of wafers at JM

Catalyst Coated Filters – Initial Results

Inconsistent and scatter results – near impermeability and breakage point

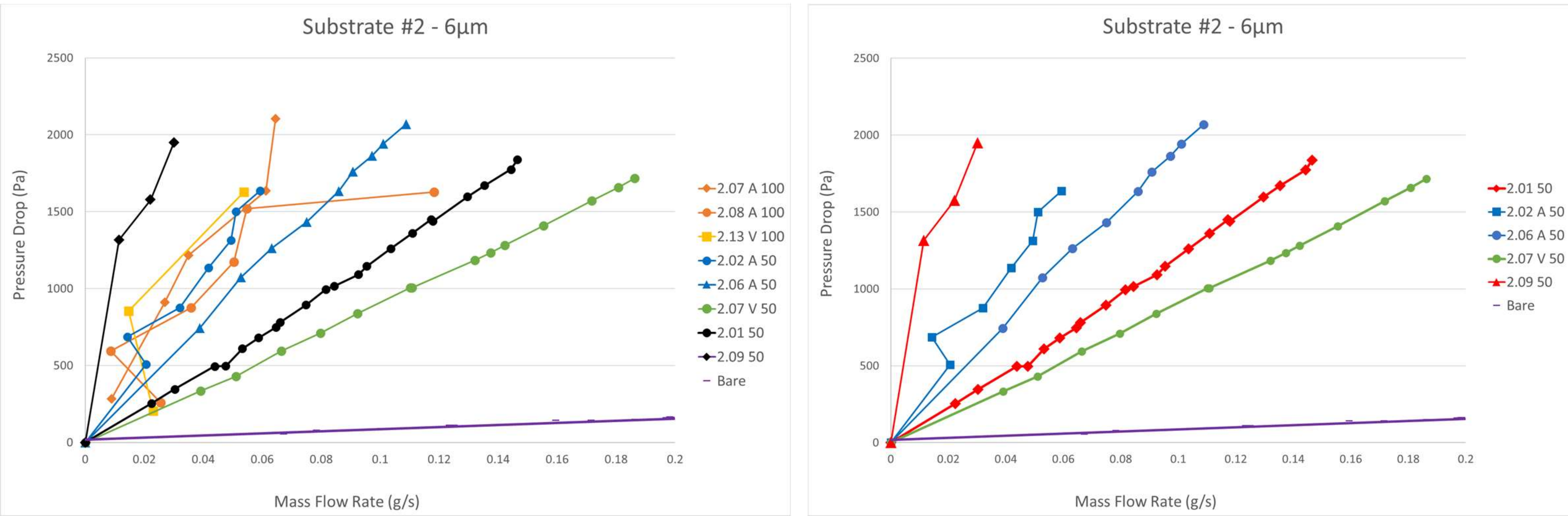

Fig 51. Results from first coated wafer attempts.

Catalyst Coated Filters – Initial Results

Attempt with smaller washcoat particle size and more controlled viscosity:

- Results show higher consistency.
- 9 wafer samples are in good agreement, all within 20% of the mean.
- There is approximately a 26% variation in permeability between samples with the highest and lowest pressure drops.
- Compared to bare wafers, this substrate exhibits a permeability around 7 times lower, leading to increased pressure drop.

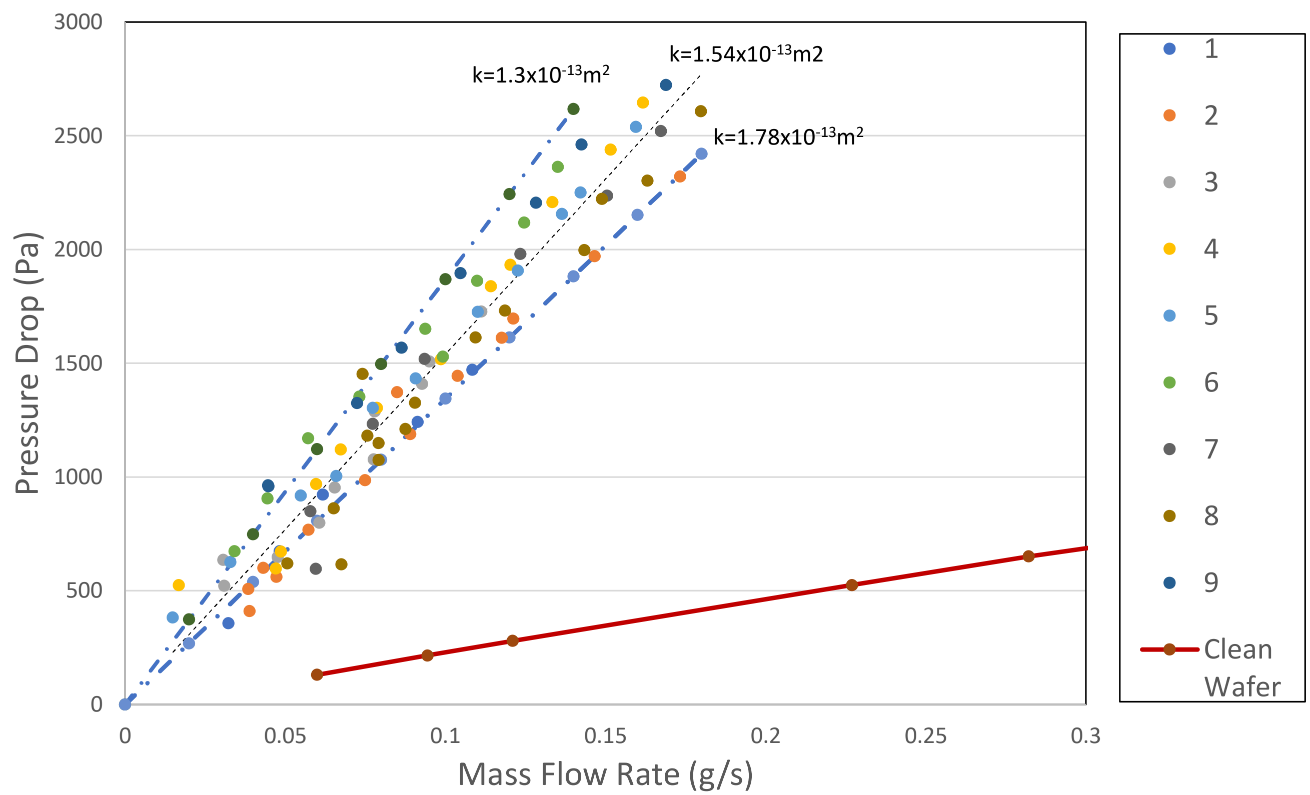

Fig 52. Results from second attempt at coated wafers.

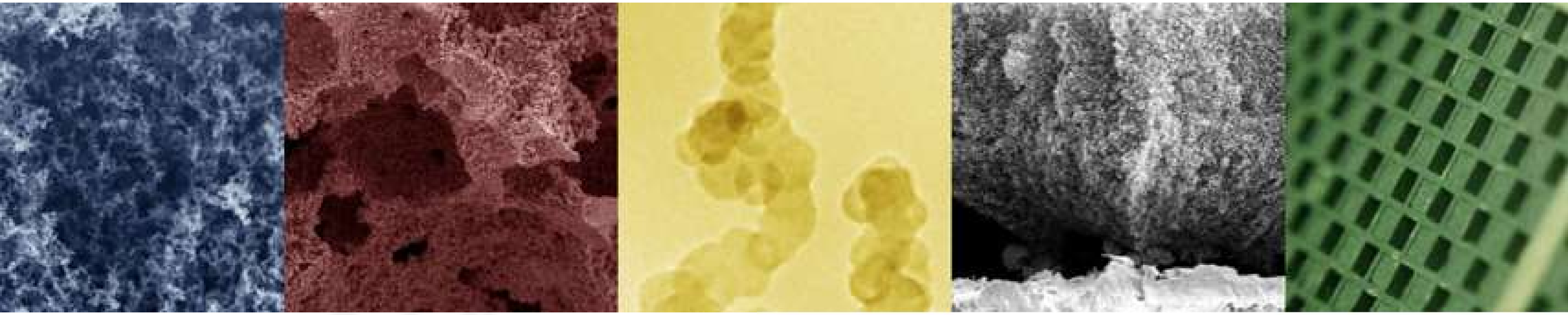

Thank you for listening

CONACT INFO:
Email: Samuelsc2@uni.coventry.ac.uk
LinkedIn: www.linkedin.com/in/callum-samuels or QR code

Johnson Matthey
Inspiring science, enhancing life

University of Leicester

The University of Nottingham

Coventry University